Thermal, structural and degradation properties of an aromatic-aliphatic polyester built through ring-opening polymerisation

Journal Name

ARTICLE

Thermal, structural and degradation properties of an aromatic-aliphatic polyester built through ring-opening polymerisation

Received 00th January 20xx,
Accepted 00th January 20xx

DOI: 10.1039/x0xx00000x

www.rsc.org/

Erlantz Lizundia*[1,2], Vishalkumar A. Makwana[3], Aitor Larrañaga[4], José Luis Vilas[2,5], Michael P. Shaver*[3]

Keywords: polyesters; ring-opening polymerization (ROP); thermal transitions; thermal stability; crystalline structure; biodegradation

The novel biodegradable aromatic-aliphatic polyester, poly(2-(2-hydroxyethoxy)benzoate, was explored through thermal analysis, X-ray diffraction, dynamic mechanical analysis and comparative bio and catalysed degradation. The polyester is a product of ring opening polymerisation (ROP) of 2,3-dihydro-5H-1,4-benzodioxepin-5-one catalysed by an aluminium salen catalyst. Thermal and mechanical characterisation showed that the polyester had a T_g of nearly 27 ºC and crystallisation ability when cooled from melt, providing an insight to potential biomedical and compatibiliser applications. These thermal and mechanical properties can be tuned by altering the polymer's molecular weight. The crystal structure has been also determined through wide-angle X-ray diffraction (WAXD). The polymer can be enzymatically degraded, but this process is slow compared to the rapid degradation by exploiting the monomer-polymer equilibrium catalysed by the aforementioned aluminium salen complex.

Introduction

As concerns about the environmental impact of plastic waste increase, there is renewed interest in the life-cycle of polymeric materials, including biodegradable polymers.[1] A focus of this has been on the development of hydrolytically and enzymatically degradable aliphatic polyesters, i.e. poly(lactic acid) (PLA), to replace commodity plastics. The narrow range of accessible properties of PLA has limited the practical uses of the green plastic, while the necessity for industrial biodegradation conditions has limited the environmental impact.[2]

Advances in monomer design have expanded the range of polymers accessible, and thus the potential applications, especially for catalyst systems with a broad monomer scope such as highly active organocatalysts[3] and selective aluminium salen complexes.[4] Baker and co-workers were pioneers in developing degradable polyesters that have added functionality to tune thermal and mechanical properties of the resultant polymer.[5] For instance, addition of an aromatic ring pendant to the backbone through the ring-opening polymerisation (ROP) of mandelide[6] produced a polyester with thermal properties similar to that of polystyrene (PS). The same polymer could be targeted through polymerisation of 5-phenyl-1,3-dioxolane-2,4-dione[7] or 5-Phenyl-1,3-dioxolan-4-one[8] to access isotactic poly(mandelic acid)s.

The paucity of research on the complementary introduction of aromaticity into the polymer backbone, rather than pendant to the main chain, through ring-opening polymerisation is surprising. Poly(ethylene terephthalate) (PET) is poorly (bio)degradable, yet is widely used due to its exceptional thermal properties, with relatively high glass transition temperatures (T_g = 67- 81 °C), low gas permeability and high chemical resistance.[9, 10] Conversely, the ortho-linked poly(ethylene phthalate) (PEP) has a lower T_g (38.2 °C)[10] and a lower degree of crystallinity (the fractional amount of crystallinity, phases where macromolecules fold together to form ordered regions, in the polymer sample expressed either as the mass fraction or as the volume fraction) due to the kinked chain induced by the ortho ester linkages.[11] While not a dominant commodity plastic, this gives PEP an advantage as a copolymer to reduce brittleness.[10] While ROP of cyclic PET oligomers has accessed PET polymers and copolymers,[12] simple monomers remain elusive as feedstocks for PET or PEP mimics. Although PET and PEP have desirable manufacturing properties, their poor degradability and leaching of phthalates raises concerns. Recycling of PET has been optimised to reduce this leaching, however harsh reaction conditions are required.[13]

We recently reported the ring-opening polymerisation of a new monomer, 2,3-dihydro-5H-1,4-benzodioxepin-5-one (2,3-DHB), to afford the aromatic-aliphatic polyester poly(2-(2-hydroxyethoxy)benzoate) (P2HEB, Scheme 1).[14] Like PEP, P2HEB

[1]*Department of Graphic Design and Engineering Projects. Bilbao Faculty of Engineering. University of the Basque Country (UPV/EHU), Bilbao 48013, Spain.*
[2]*Macromolecular Chemistry Research Group. Dept. of Physical Chemistry. Faculty of Science and Technology. University of the Basque Country (UPV/EHU), Leioa 48940, Spain.*
[3]*EaStCHEM School of Chemistry. University of Edinburgh, Joseph Black Building, David Brewster Rd, Edinburgh EH9 3FJ*
[4]*SGIker, General Research Services, University of the Basque Country (UPV/EHU), Spain.*
[5]*Basque Centre for Materials, Applications and Nanostructures (BCMaterials), Parque Tecnológico de Bizkaia, Ed. 500, 48160 Derio, Spain.*

has its aromatic ring in the ortho position, however unlike PEP it is able to undergo selective depolymerisation back to its cyclic monomer. The aluminium salen catalyst, **1**, offers control over both the polymerisation and depolymerisation of polymer through exploiting the monomer-polymer equilibrium of P2HEB.

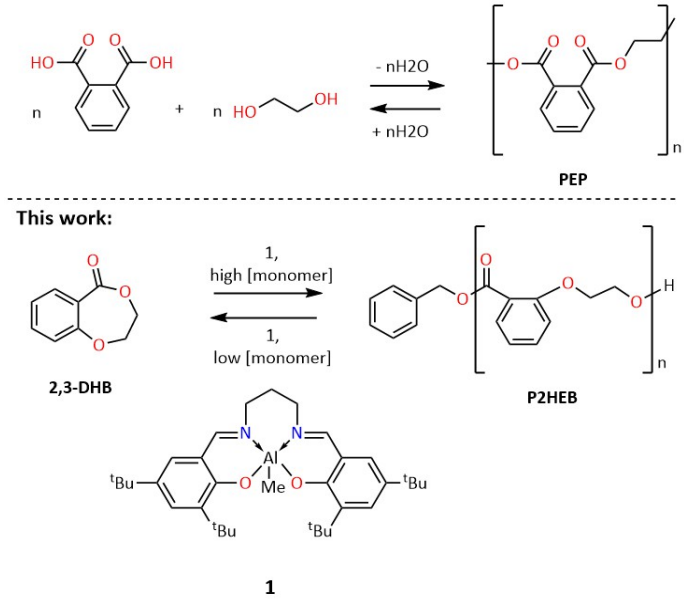

Scheme 1. Polymerisation and depolymerisation of PEP and P2HEB. Top: PEP requires harsh conditions and further purification to obtain the starting material phthalic acid after polycondensation. Bottom: P2HEB is recycled back to its monomer under mild conditions.

This paper expands on this initial communication by targeting higher molecular weight P2HEBs, characterising the thermal and mechanical properties of these new polymers, identifying their crystal structure and comparing enzymatic and catalytic degradation profiles. These new experimental findings may pave the way for the optimization of recyclable novel degradable polyesters.

Results and discussion

Homopolymerisation of 2,3-DHB

The ROP of 2,3-DHB was catalysed by aluminium salen complex **1** in toluene using a benzyl alcohol initiator, forming P2HEB of consistently low D and predictable molecular weights, even at high conversions (Table S1). Altering the monomer to catalyst ratio from $[2,3\text{-DHB}]_0:[Al]_0:[BnOH]_0$ of 100:1:1 to 500:1:1 and 1000:1:1 afforded polymers of 11,600, 40,300 and 78,600 g mol^{-1} respectively, without compromising polymerisation control or conversion.

Thermal transitions of P2HEB

The presence of thermal transitions in P2HEB was observed by differential scanning calorimetry (DSC) scans. Fig. 1a displays the 1st and 2nd heating traces obtained at a heating rate of 10 °C/min for P2HEB (see Fig. S1 and Table S2 for the effect of heating rate on the thermal transitions). It could be seen that during the 1st heating scan P2HEB undergoes a heat enthalpy change centred at 26.5 °C which is identified with the glass transition temperature (T_g). Further temperature increase leads to a single well-defined endothermic event in the 60-80 °C range (centred at 68.8 °C) associated with the melting of P2HEB crystals (T_m). This well-defined melting curve denotes the presence of a narrow distribution of crystals within the sample.[15] The enthalpy of fusion or ΔH_m, determined as the area under the melting curve, has been measured to be 29.8 J/g. No cold-crystallisation is observed between both T_g and T_m upon heating, suggesting that the sample does not further crystallize.

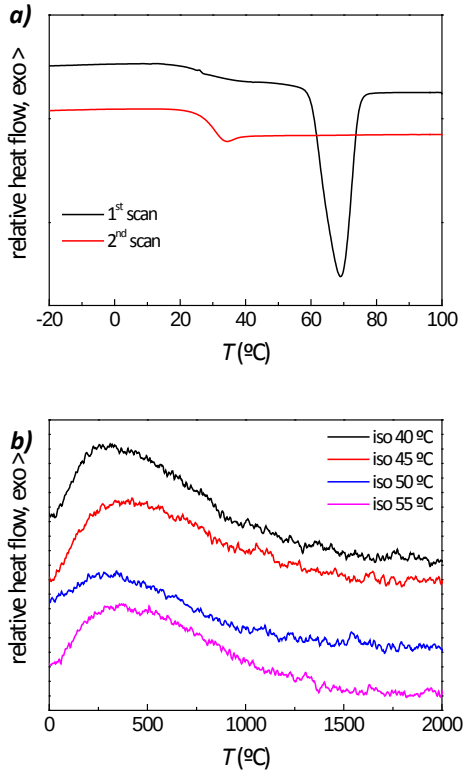

Fig. 1. DSC 1st and 2nd heating traces of P2HEB (a) and isothermal crystallisation traces obtained at different temperatures (b).

Once P2HEB has been melted, it has been quenched down to -30 °C and a second heating scan was applied. Surprisingly, this second scan only shows the characteristic second order transition at 30.8 °C associated with the T_g, indicating that once the polymer has been melted it cannot be crystallized upon cooling. Therefore, the initially semicrystalline P2HEB was turned into totally amorphous material displaying a single thermal transition event (T_g). To discard the occurrence of any thermal degradation event during these DSC heating scans, P2HEB has been subjected to a heating scan up to 100 °C and its molecular weight (determined by gel permeation chromatography) and microstructure (by proton nuclear magnetic resonance, ^{1}H NMR) was compared to that corresponding to the original material. As shown in Table S3 and Fig. S2, both the number average molar mass (M_n) and ^{1}H NMR spectrum indicates that the original structure of P2HEB is kept intact during DSC analysis.

To seed further light on the occurring thermal transitions in P2HEB, isothermal treatments at four temperatures between T_g and T_m have been carried out. Fig. 1b reveals the crystallisation

exotherms obtained when P2HEB is cooled down from the melt to 40, 45, 50 and 55 °C. No noticeable differences in the crystallisation behaviour are found, being the crystallisation half time ($t_{1/2}$) and enthalpy barely unchanged at ~9 minutes and 1.1-1.3 J/g respectively. This slow kinetics and small amount of crystallisation enthalpy observed further confirm the low crystallisation ability of P2HEB when it is cooled from the melt.

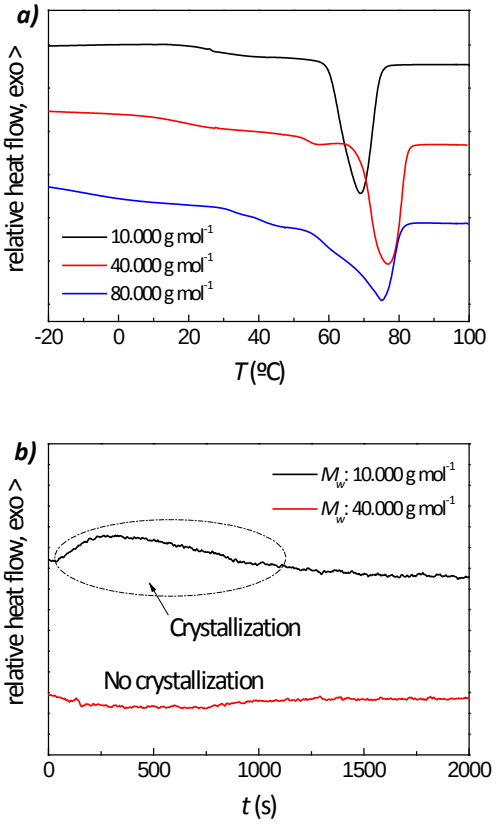

Fig. 2. DSC 1st heating traces of P2HEB depending on the molecular weight (a) and isothermal crystallisation traces obtained at T_c=40°C for P2HEB of 10.000 and 40.000 g mol^{-1}(b).

The effect of the molecular weight on the thermal transitions and crystallisation behaviour of P2HEB is shown in Fig. 2. Glass transition temperature is slightly shifted toward higher temperatures, while T_m increases up to 76.8 °C for the P2HEB having 40,000 g mol^{-1}. As denoted by the non-existence of exothermic peak when the P2HEB 40,000 g mol^{-1} is cooled down to 40 °C from the melt in Fig.2b, high-molecular weight sample crystallize even less than low-molecular weight P2HEB. These results arise from the higher molecular mobility of shorter chains which, in comparison with longer chains having the same chemical nature, present lower and higher crystallisation capacity.[16, 17]

Overall, it is observed that P2HEB displays a very different crystalline behaviour in the nascent form and after melting, which has been already found for materials such as ultra high molecular weight polyethylene (UHMWPE),[18] polyoxymethylene,[19] and heterotactic polylactide.[20] Nascent P2HEB, directly obtained after ROP, is obtained in powder form and displays a high crystallinity because polymerization reaction facilitates its crystalline growth. During ROP, P2HEB chains are organised into regular segments because these chains can disentangle and rearrange into large regular crystals by chain sliding diffusion.[21] It has been shown that ROP conditions result critical in this process; while the presence of catalyst supports act as impurities which lower the energy barrier to crystallisation, polymerisation variables such as concentration, temperature, pressure and medium also affect crystallization process.[22] On the contrary, when P2HEB is heated above 80 ºC its nascent crystalline structure is lost. As indicated by DSC traces in Fig. 1, upon cooling from the melt, P2HEB recrystallizes with a disordered structure, yielding a crystallinity degree notably lower than at its nascent state. A similar behaviour has been found by Jauffrès et al. for UHMWPE during the high velocity compaction (HVC) processing.[19]

Thermal degradation of P2HEB

In order to analyse the thermal degradation behaviour of P2HEB, thermogravimetric analysis (TGA) under nitrogen atmosphere has been employed. Fig. 3 shows the thermogravimetric (left) and weight loss rates (right) of P2HEB (11,000 g mol^{-1}) for four different heating rates, whereas the characteristic temperatures of thermal degradation are shown in Table 1. It is observed that for all the heating rates, thermal degradation of P2HEB process in a well-defined main step comprising ~91% of the whole weight loss, which is followed by a less marked second degradation at higher temperatures. Overall, it is seen that thermal degradation is delayed as heating rate increased. At a heating rate of 1 °C/min the onset

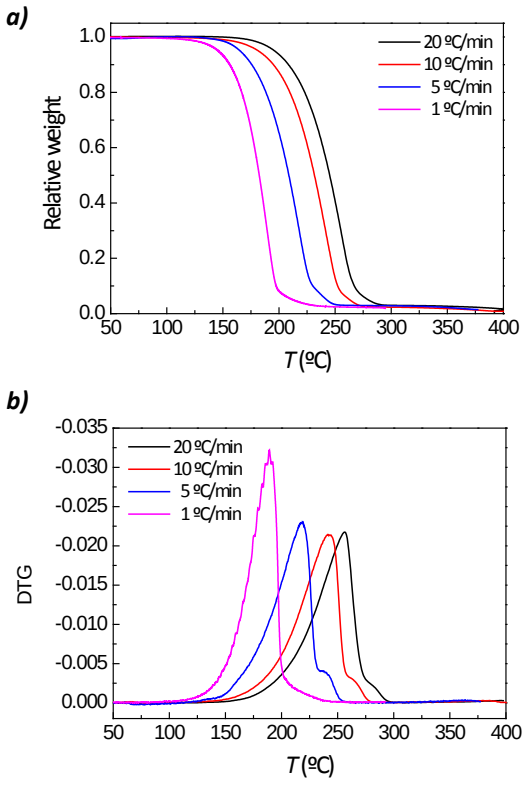

Fig. 3. Thermogravimetric traces (a) and weight lost rates (b) obtained at different heating rates under N_2 atmosphere.

	1 (ºC/min)	5 (ºC/min)	10 (ºC/min)	20 (ºC/min)
$T_{5\%}$ (ºC)	145.6	165.8	181.6	196.4
T_{peak} (ºC)	188.9	218.2	242.1	256
DTG	-0.0311	-0.0229	-0.0214	-0.0217

Table 1. Main thermodegradation parameters of P2HEB.

of thermal degradation (determined by the first 5 wt.% weight loss, $T_{5\%}$) takes place at 145.6 ºC, which is increased up to 196.4 ºC when heating rate is of 20 ºC/min. Similarly, the maximum degradation rate (T_{peak}) is shifted from 188.9 to 256 ºC when heating rate increases from 1 to 20 ºC/min. Additionally, TGA traces are shifted by about 6 ºC when the molecular weight of P2HEB increases from 11,000 to 80,000 g mol^{-1} (see Fig. S3).

It is worthy to note that the thermal degradation occurs notably earlier in the case of P2HEB than in the case of other polyesters. For instance, for a heating rate of 10 ºC/min, the onset of thermal degradation of poly (L-lactide) (PLLA) has been found to be 290.5 ºC,[23] while $T_{5\%}$ occurs at 339.8 and 274.5 ºC in the case of polycaprolactone (PCL) and poly(lactide-co-caprolactone) (PLCL) respectively.[24] In this respect, the application range of this polymer should be limited to low temperature environments (<100 ºC) and a careful attention should be paid during the melt processing of P2HEB.

In order to quantify the kinetic parameters of thermal degradation, TGA experiments were conducted at 1, 5, 10 and 20 ºC/min under N_2 atmosphere. The activation energy (E) associated to the thermal degradation has been computed according to *Kissinger´s* equation, which requires obtaining the temperature values that occur at the maximum degradation rate (T_{max}). The activation energy is then calculated from the slope of $\ln(\beta/T^2_{max})$ as a function of $1/T_{max}$:[25]

$$\ln\frac{\beta}{T^2} = \left[\ln\left(\frac{AE_a}{R(\alpha)}\right)\right] - \frac{E_a}{RT} \qquad (1)$$

being β is the heating rate, A the pre-exponential factor, α_{max} the maximum conversion, n is the reaction order and R is the universal gas constant (8.314 J/K mol). In the light of Kissinger´s equation, the activation energy of thermodegradation process for low-molecular-weight P2HEB (10.000 g mol^{-1}) has been found to be 79.7 ± 6.5 kJ mol^{-1}. It is observed that E_a slightly increases up to 84.1 ± 9.3 kJ mol^{-1} for higher molecular weight P2HEB (80.000 g mol^{-1}), similarly to that occurs to other polymers such as polystyrene and poly(phenylene sulfide ether).[26,27] These values remain well-below from the typical activation energies found for other polyesters such as PLLA (100.8-163.8 kJ mol^{-1}),[23,24] PCL (228.9 kJ mol^{-1}) or PLCL (136.3 kJ mol^{-1}) confirming the relatively low thermal stability of P2HEB.[24]

Dynamic mechanical properties

The determination of how the dynamic mechanical properties of P2HEB change with temperature results a key issue for its prospective application. To that end, the dynamic mechanical properties of P2HEB have been investigated by dynamic mechanical analysis (DMA). P2HEB films being 200 µm thick have been obtained by solvent casting method using chloroform as a solvent (see Fig. S4 for solubility tests). Because the as-polymerised polymer presents a powder form that cannot be mechanically tested, the dynamic mechanical properties of casted films obtained after the dissolution of P2HEB and evaporation of chloroform are here shown (which removes the original structure of the nascent P2HEB). As shown in Fig. S5, firstly a dynamic strain sweep experiment over the 0.001-10 % range has been conducted to determine the strain range in which the observed viscoelastic properties remain independent of imposed forces. Accordingly, P2HEB´s linear viscoelastic region (LVR) at temperatures below its T_g (experiments were carried out at 0 ºC), identified as the onset of the $E´$ storage modulus drop as a consequence of the simple overstrain, is found to be at 0.4 %, indicating that further deformations destroy the elastic structure of P2HEB.

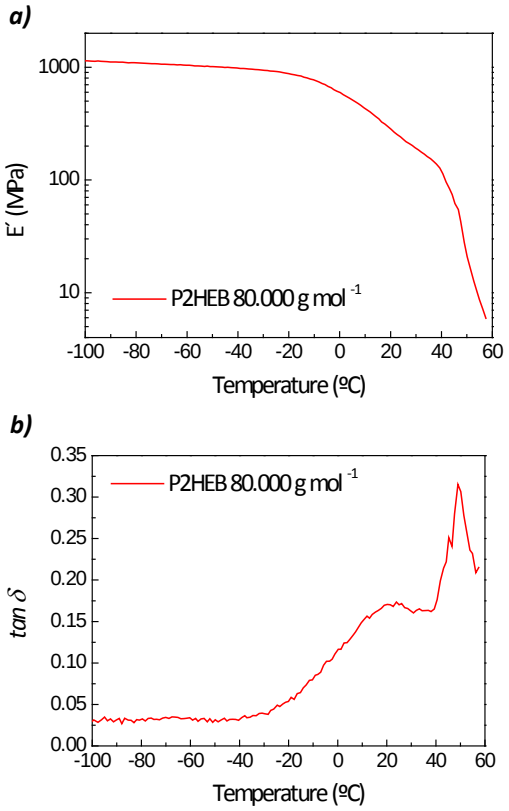

Fig. 4. Dynamic mechanical storage modulus vs temperature (a) and tan δ vs temperature (b) plots for P2HEB.

Fig. 4 displays the dynamic mechanical storage modulus ($E´$) and loss tangent ($tan\ \delta$) in the temperature range of -100 to 60 ºC for P2HEB having 80,000 g mol^{-1}. The $tan\ \delta$ damping factor indicates the way the material loses energy to molecular rearrangements and internal friction and is calculated as the ratio between the loss modulus ($E´´$) and the storage modulus. When $tan\ \delta$ takes a zero value, the material would be completely elastic, while large $tan\ \delta$ values are indicative of a highly viscous material. It is observed that at low temperatures P2HEB behaves as a rigid body and presents a storage modulus of about 1050 MPa, which is almost independent on the applied

temperature (glassy zone). This value is about half when compared with traditional petro-based polymers such as poly (methyl methacrylate) (PMMA) or other polyesters such as PLLA.[28,29] It is seen that *E´* notably decays as temperature is increased from -20 to 40 ºC (coinciding with the *tan δ* rising), to dramatically drop when it is heated above ~42 ºC. The first process where storage modulus decays occurs because of the sudden molecular mobility increase of P2HEB induced upon heating and is ascribed to α relaxation mode, or in other words, to the glass transition. At this point the polymer shows rubbery properties instead of a glassy behaviour and suffers an increase in viscosity. A maximum value of 0.17 in *tan δ* increases has been observed, which is ten times smaller than that usually found for other polyesters such as PLLA.[29] As denoted by the low *tan δ* value, it could be stated that the contribution of the storage modulus in P2HEB is higher than that of the loss modulus. This fact arises from its elastic character rather than viscoelastic one. This non-efficient process of energy dissipation may result from the presence of highly ordered domains within the structure which provide act as confining regions that provide stiff properties to the whole material.[30,31] Further temperature increase results in the melting of P2HEB crystals, the polymer undergoes a flow process and the *E´* dramatically decays to a few MPa (*tan δ* increases). It is worthy to note that as denoted by the maximum in the loss tangent (*δ*) (Fig. 5b), the T_g is centred at 23 ºC, which correlates well with the T_g values obtained through DSC. As a result of the vicinity of both T_g and T_m, P2HEB does not show the rubbery plateau found for many polymers. This marked *E´* modulus decrease near physiological temperature (37 ºC) highlights the potential of P2HEB to be used for biomedical applications.

Crystalline structure of P2HEB

P2HEB crystal has been investigated through wide-angle X-ray diffraction (WAXD). As shown in Fig. 5, the obtained X-ray diffraction data show a crystalline structure for the compound. Preliminary identification of the initial phase was evaluated using the Powder Diffraction File (PDF) database. PANalytical X´Pert High Score program was used for contrast the Miller indexing; the obtained results are not in good agreement with any known phase. The chemical configuration was tested using the CSD database Cambridge Crystallographic Data Centre (CCDC). http://www.ccdc.cam.ac.uk without any coherent results. The first XRD signal positions of the profile were extracted using the peak-fit option of the WinPLOTR and were assigned using the TREOR program for indexing unknown powder patterns. The obtained results indicate Tetragonal symmetry and *a*=*b*=7.48 Å *c*=23.28 Å for the unit cell parameters. The diffraction data of the sample was fitted using the FULLPROF program.[32-34] In the initial profile refinement the unit cell parameters, peak shape (pseudo-Voigt), background, systematic 2θ shift, Cagliotis function U,V,W half-width parameters for the profile and asymmetry parameters were refined (Fig. 6).

The obtained results show a good agreement between the experimental and calculated data, the final reliability factors, were Rp: 12.8, Rwp: 13.1, Rexp: 3.14, Chi2: 17.4 and Bragg R-factor: 0.206. The obtained final unit cell parameters were a=b=7.494(2) and c=23.19(1)A. In the space group determination process from the tetragonal symmetry the hkl conditions give as an appropriate result the P$4_2/nmc$ (137) space group, nevertheless the intense overlap of the diffraction signals at high angles (>20º2θ) give small *hkl* correlation to be completely sure about the systematic absences. Concerning the structure, the clear and sharp XRD signals at low angles indicate high crystalline compound for high spacing (long range crystal structure), in the other hand the high broadening for the coherently diffracting domains at higher angles points to a probably polymer chain conformational disorder. It is worthy to note, that as depicted in Fig. S6, the crystal structure remains unchanged for different molecular weight P2HEBs.

The crystalline behaviour of the P2HEB was restricted to the (00L) and (10L) planes indicating a high crystalline lamellar structure of about 20x30 nm. It is observed that nascent P2HEB exhibits a highly crystalline nanostructure characterized by a poorly ordered arrangement of small crystallites in the [0k0] direction as a consequence of the topological constrains for the amorphous component.[19] A complete melting of the sample leads to the lost of these nascent phase specificities (high crystallinity and topological constrains in one direction). Overall, X-ray diffraction data suggest that while melt-crystallized exhibits an amorphous structure, nascent P2HEB shows a very particular structure formed of lamellae of crystal "blocks" that do not extend themselves in one direction (0k0).

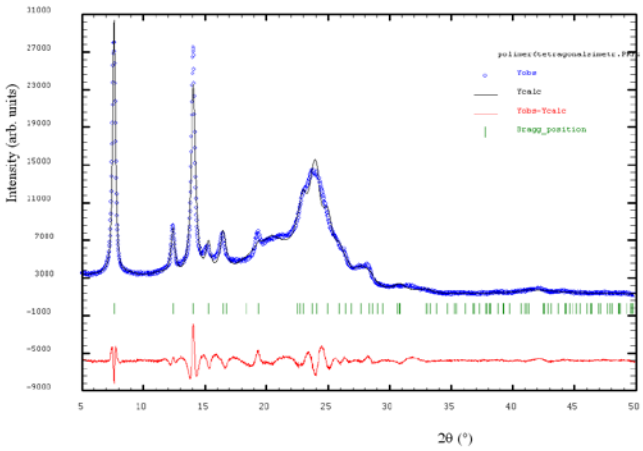

Fig. 5. X-ray diffraction full profile refinement. Circles denote experimental points and upper solid lines the calculated profile. Theoretical peak positions (vertical sticks) and difference line is shown in the bottom of the pattern.

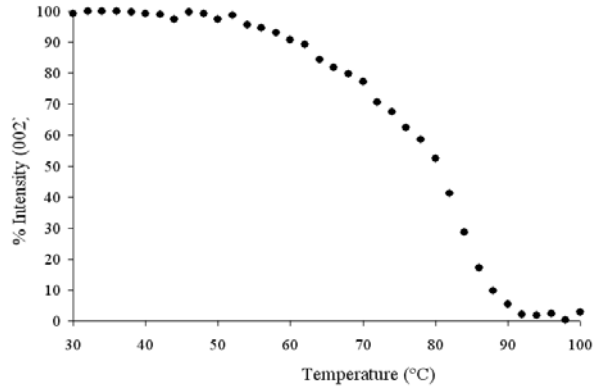

Fig. 6. Normalized intensity area of the (002) plane upon heating.

High temperature X-ray patterns were recorded in order to determine how the crystalline structure changes upon heating as this may correlate with the melting of P2HEB crystals. As shown in Fig. 6, the normalized intensity area corresponding to the main (002) plane decreases at temperatures above 55 °C as a result of the crystal structure loss induced by the melting process. It is observed that at 85 °C a fully amorphous halo is recorded, where the relative intensity drops below 5 %. This result is in line with the T_m of 68.8 °C measured by DSC and shown in Fig. 1.

Enzymatic and chemical degradation studies of P2HEB

Enzymatic degradation studies were carried out on the aforementioned polymer films of P2HEB for the two highest molecular weights, as consistent film formation was challenging with low molecular weight samples. Films were prepared from solution casting P2HEB chloroform solutions onto PTFE plates affording 100 µm thick films after solvent evaporation. The respective films were cut into 1 cm^2 squares and exposed to proteinase K enzyme in a tris-HCl buffer.

The enzymatic degradation was monitored via molecular weight loss using GPC (Fig. 7 and Fig. S8). GPC traces show a clear shift towards lower hydrodynamic volumes, indicating a decrease in molecular weight. Both 40,000 and 80,000 g mol^{-1} P2HEB polymer films show the same percentage change in hydrodynamic volume, and retained the same low dispersity of the starting polymers (Table S4 and S5).

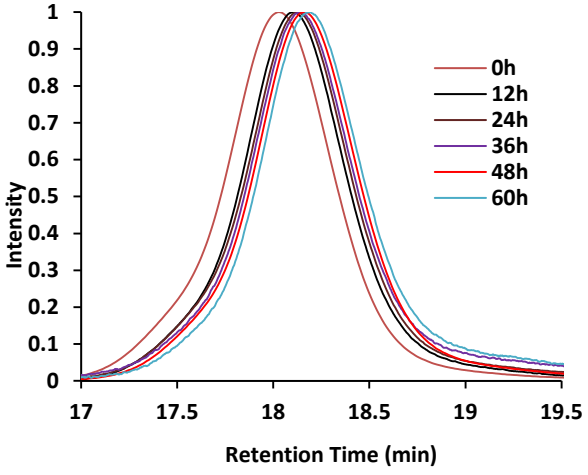

Fig. 7. GPC trace of P2HEB of molecular weight 40 kDa with their dispersity at 12-hour intervals to show the decrease in molecular weight as the degradation studies proceed.

^{1}H NMR spectroscopy was used to more accurately track the kinetics of this degradation (Fig. 8). As with GPC, both films showed the same degree of degradation, with a 39% decrease in molecular weight over 60 h. Note that the discrepancy of molecular weight values obtained by GPC and ^{1}H NMR is due to the poor solubility of P2HEB in THF, meaning that accurate dn/dc values cannot be obtained, so reported molecular weights are versus polystyrene standards. The similarity of the linear correlations between percentage weight loss and time suggests an independence of molecular weight on the rate of degradation.

Enzymatic degradation of P2HEB is significantly faster than for PET, evidenced by a higher percentage weight loss.[9] The ester linkage in P2HEB can preferentially orientate itself 90° to the phenyl ring, with the resulting highly kinked units along the polymer backbone[11] leading to a higher degree of chain mobility, lower crystallinity and easier access for enzyme attack.[10] Conversely, enzymatic degradation of P2HEB is much slower than for atactic poly(lactic acid).[35,36] The absence of an aromatic ring to restrict the ester linkages allows for PLAs higher degradation rates.

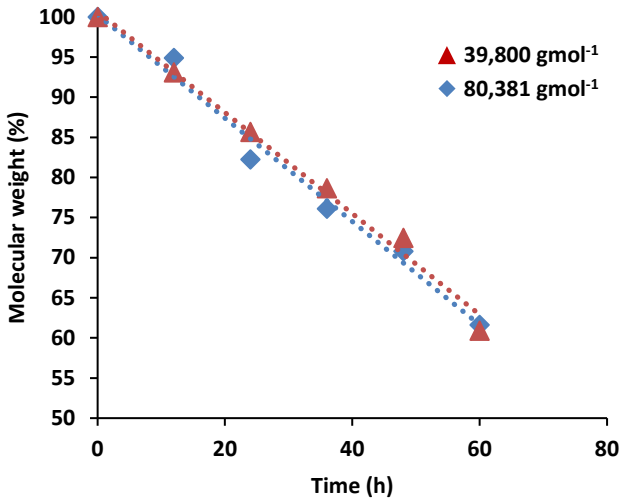

Fig. 8. Percentage of molecular weight loss as a function of time, obtained by ^{1}H NMR, showing zero order kinetics.

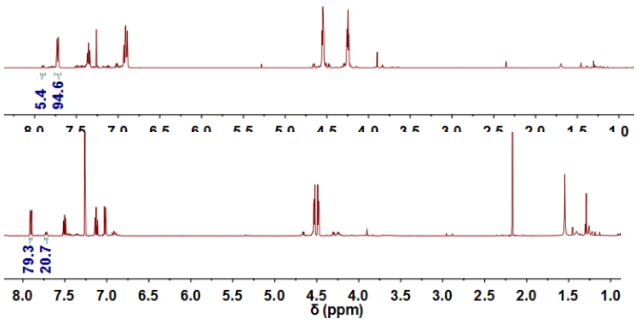

Fig. 9. Comparison of one of the aryl protons in P2HEB to show the monomer peak at 7.8 ppm increasing upon chemical degradation. Top: P2HEB and Bottom: Depolymerised P2HEB back to its cyclic monomer (2,3-DHB) after 1 hour.

While enzymatic degradation is slow, these systems were designed to promote Lewis-acid catalysed degradation. Degradation of P2HEB films of all three molecular weights were investigated in the presence of aluminium salen **1**. While P2HEB degradation is hampered at room temperature by poor solubility in organic solvents, degradation at 70 °C in toluene is rapid. The degree of degradation after 1h is independent of molecular weight, with 80% molecular weight loss for each sample (Fig. 9). No difference in degradation profile was observed if samples were processed into films, isolated as powders, or if degradation was conducted *in situ* after polymerisation, expanding upon the solution degradation studies we earlier reported.[14] Once again, depolymerisation was selective, with monomer being the only product formed during catalysed depolymerisation.

The rapid recycling to monomer is a promising new route to rethink the polymer life-cycle, especially when compared to much slower enzymatic degradation kinetics. Catalytic degradation reforms the original cyclic ester monomer, which can be used in repolymerisation processes without further processing. The rapid rates of degradation and elimination of monomer synthesis steps make it a promising re-think of polymer degradation that we are now exploring with other polymer systems.

Conclusions

The biodegradable and catalytically degradable aliphatic-aromatic polyester P2HEB has been thermally and mechanically characterised, with properties similar to that of poly(ethylene phthalate). Two different glass transition temperatures were observed over two DSC scans of P2HEB, suggesting sluggish crystallisation ability, exacerbated at higher molecular weights. The low crystallisability and T_g of P2HEB accessed characteristic rubber-like properties at physiological temperatures; below the T_g the polymer behaved as a rigid body, albeit with a relatively low dynamic mechanical storage modulus. WAXD was used to further explore P2HEB semi-crystallinity, with regions of high crystallinity and conformational disorder below 85 °C. A zero-order dependence of molecular weight on a slow enzymatic degradation, while catalysed degradation to cyclic monomer was rapid and selective even from polymer films. These characteristics suggest potential applications of P2HEB in biomedical applications, as a mid-block in thermoplastic elastomers, and as a component of polymer blends.

Experimental

General considerations and materials

Polymerisations were carried out under a nitrogen atmosphere in a Vigor glovebox equipped with a −35 °C freezer and [H2O] and [O2] detectors. Dispersities were determined using gel permeation chromatography (GPC) in THF at a flow rate of 1 mL min^{-1} at 35 °C on a Malvern Instruments Viscotek 270 GPC Max triple detection system with 2 x mixed bed styrene/DVB columns (300 × 7.5 mm). Molecular weights were also determined by ^{1}H NMR spectroscopy by integration of polymer vs initiator resonances in $CDCl_3$ on a Bruker Asance 500 MHz spectrometer.

Benzyl alcohol (BnOH) was dried for 24 hours under reflux with calcium hydride and distilled under an inert atmosphere. Toluene was collected from an Innovative Technologies solvent purification system consisting of columns of alumina and copper catalysts. Toluene and BnOH were degassed via three freeze-pump-thaw cycles prior to use. 2,3-Dihydro-5H-1,4-benzodioxepin-5-one (2,3-DHB) was recrystallised three times from EtOAC: Hexanes (50:50) prior to it being dried under vacuum and sublimed at 60 °C for 18 hours.[14] Aluminium salen **1**, was synthesised following a modified literature procedure.[37,38].

Synthesis of P2HEB

Following a modified literature procedure,[14] 2,3-DHB (1.05 g, 6.38 mmol), Aluminium salen **1** (42.9 mg, 0.09 mmol), BnOH (9.4 µL, 0.09 mmol) and toluene (0.3 mL) were added to an ampoule. The reaction was heated at 60 °C for six hours. The polymerisation was quenched with 0.5 mL of a 10% methanol in dichloromethane solution and precipitated in cold methanol to afford an off-white solid. ^{1}H NMR (500 MHz, $CDCl_3$): δ 7.72 (dd, 1H, Ar**H**), 7.35 (dd, 1H Ar**H**), 6.94–6.86 (m, 2H, Ar**H**), 5.29 (s, 2H, PhC**H$_2$**O) 4.55 (t, 2H, C(O)OC**H$_2$**CH$_2$O), 4.25 (t, 2H, C(O)OCH$_2$C**H$_2$**O). ^{13}C NMR (126 MHz, $CDCl_3$): δ 166.10 (**C**(O)OR), 158.56, 133.67, 131.87, 120.96, 120.81, 114.18 (Ar), 67.37 (C(O)OCH$_2$**C**H$_2$O), 62.97 (C(O)O**C**H$_2$CH$_2$O).

Differential scanning calorimetry (DSC)

The thermal behaviour of samples was determined using a Mettler Toledo DSC 822e calorimeter under nitrogen atmosphere (30 mL/min). Samples of 7 mg were sealed in an aluminium pan, heated from -30 to 100 °C at a rate of 10 °C/min and held at 100 °C for 2 minutes to remove previous thermal history. Samples have been cooled to different crystallisation temperatures (Tc= 40, 45, 50 and 55 °C) at 50 °C/min and held at this temperature for 200 minutes to ensure that crystallisation process is completed. A subsequent heating scan at 10 °C/min was applied from -20 °C to the samples in order to determine the thermal transitions.

Thermogravimetric analysis (TGA)

Thermal degradation behaviour was studied by means of thermal gravimetric analysis (DTG-60 Shimadzu) in alumina pans with nitrogen flux of 20 mL/min for each sample (9 ± 1 mg). Samples were heated from room temperature to 500 °C at 1, 5, 10 and 20 °C/min. Thermodegradation products analysis has been performed using a Thermo Nicolet Nexus 670 FTIR spectrophotometer connected through an interface to the thermobalance. FTIR scans were taken every 16s.

UV-Vis spectroscopy (UV-Vis)

UV-Vis absorption spectra were recorded with a Shimadzu MultiSpec-1501 spectrophotometer. Total transmittance experiments have been analysed in the range of 190 to 800 nm with a sampling interval of 1 nm and 25 accumulations. A P2HEB thin film was obtained by melting 20 mg of polymer between two plain glass microscope slides and allowing to cool down to room temperature naturally.

Gel permeation chromatography (GPC)

Dispersity was determined using a Waters 1515 gel permeation chromatograph (GPC). Samples were dissolved in chloroform at a concentration of 2 mg mL^{-1} at 298 K. Calibration was obtained using narrowly-distributed polystyrene standards and chloroform as the mobile phase at a flow rate of 0.5 mL/min.

Wide angle X-Ray diffraction (WAXD)

X-ray powder diffraction patterns were measured using a Bruker D8 Advance diffractometer equipped with a Cu tube, Ge(111) incident beam monochromator (λ = 1.5406 Å) (fixed slit 1 mm) and a Sol-X energy dispersive detector (fixed slit 0.06 mm). The sample was mounted on a zero background silicon wafer embedded in a generic sample holder. Data were collected from 5 to 50° 2θ (step size = 0.02 and time per step = 100 s, total time 60 h) at RT. A fixed divergence and antiscattering slit (1°) giving a constant volume of sample illumination was used. The high temperature X-ray patterns of the sample was registered on a Bruker D8 Advance diffractometer operating at 30 kV and 20 mA, equipped with a Cu tube (λ = 1.5418 Å), a Vantec-1 PSD detector, and an Anton Parr HTK2000 high-temperature furnace with a direct sample heating Pt sample holder. The powder patterns were recorded in 2θ steps of 0.033 ° in the 5 ≤ 2θ ≤ 37 range. The sample was measured heating and cooling in the 30 – 100 °C range, each 2 °C at 10 °C/min.

Nuclear Magnetic Resonance (NMR)

Room temperature nuclear magnetic resonance (NMR) was conducted by dissolving 10 mg of P2HEB in 0.8 mL of deuterated chloroform ($CDCl_3$). Experiments were carried out in a Bruker Avance-II 300 MHz spectrometer.

Dynamic Mechanical Analysis (DMA)

Dynamic mechanical analyses were performed on a DMA/SDTA861 analyzer (Mettler- Toledo) in tensile mode. 200 µm thick samples (4 mm wide and 5.5 mm long) were obtained through solvent-casting method. Curves displaying storage modulus (*E´*) and the energy loss (*tan δ*) were recorded as a function of temperature at a heating rate of 3 °C/min, a frequency of 1 Hz and displacement of 5 µm (or 0.1% strain, within the Linear Viscoelastic Region as depicted in the inset of Fig. S5).

Preparation of P2HEB polymer films

P2HEB (0.50 g) of molecular weight 40,000 and 80,000 $gmol^{-1}$ were dissolved in 6 mL of chloroform and pipetted, avoiding bubble deposition, onto a PTFE plate with a diameter of 7.4 mm. The PTFE plate was covered with a glass lid and placed on a balance to allow even evaporation of the solvent to form a film of 0.1 mm thickness.

Enzymatic degradation of P2HEB

Following a modified literature procedure,[35] the respective polymer films (1 cm squares) were placed in separate vials consisting of Tris-HCl buffer (5 mL, 50 mM, pH 8.6) and 1 mg of proteinase K. The vials were placed in an incubator at 37 °C on a rotary shaker set to 250 rpm. The study was carried out over 60 hours, analysing three separate replicates of each film every 12 hours. Analysis was carried out by removing the film from the buffer solution, rinsing it with distilled water and drying in vacuum at room temperature over phosphorus pentoxide until constant mass was obtained.

Chemical degradation of P2HEB

Following a modified literature procedure,[14] P2HEB of the respective molecular weights (0.0045 mmol) and MeAl[salen] (0.0045 mmol) were dissolved in toluene (0.003 M) in an ampoule. The ampoule heated to 70 °C for one hour.

Acknowledgements

The authors would like to thank the University of Edinburgh, EPSRC, Soft Matter and Functional Interfaces Centre for Doctoral Training and the Marie-Curie Actions Programme (Grant FP7-PEOPLE-2013-CIG-618372). Authors also thank the Basque Country Government for financial support (IT718- 13).

References

1. A. Frydrych, Z. Florjańczyk, M. Charazińska and M. Kąkol, *Polym. Degrad. Stab.*, 2016, **132**, 202-212.
2. O. Martin and L. Averous, *Polymer*, 2001, **42**, 6209-6219.
3. A. M. Goldys and D. J. Dixon, *Macromolecules*, 2014, **47**, 1277-1284.
4. E. D. Cross, L. E. N. Allan, A. Decken and M. P. Shaver, *J. Polym. Sci., Part A: Polym. Chem.*, 2013, **51**, 1137-1146.
5. T. L. Simmons and G. L. Baker, *Biomacromolecules*, 2001, **2**, 658-663.
6. T. Liu, T. L. Simmons, D. A. Bohnsack, M. E. Mackay, M. R. Smith and G. L. Baker, *Macromolecules*, 2007, **40**, 6040-6047.

7. I. J. Smith and B. J. Tighe, *Macromol. Chem. Phys.*, 1981, **182**, 313-324.
8. S. A. Cairns, A. Schultheiss and M. P. Shaver, *Polym. Chem.*, 2017. DOI: 10.1039/C7PY00254H
9. R. J.Muller, H. Schrader, J. Profe, K. Dresler and W. D. Deckwer, *Macromol. Rapid Commun.*, 2005, **26**, 1400-1405.
10. S. W. Lee, M. Ree, C. E. Park, Y. K. Jung, C. S. Park, Y. S. Jin and D. C. Bae, *Polymer*, 1999, **40**, 7137-7146.
11. A. E. Tonelli, *J. Polym. Sci., Part B: Polym. Phys.*, 2002, **40**, 1254-1260.
12. D. J. Brunelle, J. E. Bradt, J. Serth-Guzzo, T. Takekoshi, T. L. Evans, E. J. Pearce and P. R. Wilson, *Macromolecules*, 1998, **31**, 4782-4790.
13. G. P. Karayannidis and D. S. Achilias, *Macromol. Mater. Eng.*, 2007, **292**, 128-146.
14. J. P. MacDonald and M. P. Shaver, *Polym. Chem.*, 2016, **7**, 553-559.
15. L. H. Sperling, *Introduction to Physical Polymer Science*, Blackwell Science Publishing, Psney Mead, Oxford, England 2006.
16. J. L.Carvalho, S. L. Cormier, N. Lin and K. Dalnoki-Veress, *Macromolecules*, 2012, **45**, 1688-1691.
17. S. Andjelić and R. Scogna, *J. Appl. Polym. Sci.*, 2015, **132**, 1-15.
18. S. Rastogi, D. R. Lippits, G. W. M. Peters, R. Graf, Y. Yao and H. W. Spiess, *Nat. Mat.*, 2005, **4**, 635-641.
19. D. Jaiffrès, O. Lame, G. Vigier and F. Doré, *Macromolecules*, 2008, **41**, 9793-9801.
20. C. Romain, B. Heinrich, S. B. Laponnaz and S. Dagorne, *Chem. Comm.*, 2012, **448**, 2213-2215.
21. S. Yamazaki, M. Hikosaka, A. Toda, I. Wataoka and F. Gu, *Polymer* 2002, **43**, 6585.
22. T. F. L. McKenna, A. D. Martino, G. Weickert and J. B. P. Soares, *Macromol. React. Eng.* 2010, **4**, 40–64.
23. E. Lizundia, J. L. Vilas and L. M. León, *Carbohydr. Polym.*, 2015 **123**, 256-265.
24. A. Larranaga, S., Petisco and J. R. Sarasua, *Polym. Degrad. Stab.*, 2013, **98**, 1717-1723.
25. H. E. Kissinger, *Anal. Chem*, 1957, **29**, 1702-1706.
26. B. V. Kokta, J. L. Valade and W. N. Martin, *J. Appl. Polym. Sci.* 1973, **17**, 1-19.
27. A. Q. Gu, Z. L. Yu and Y. B. Li, *J. Appl. Polym. Sci.,* 2009, **114**, 911-918.
28. E. Erbas, A. Kiziltas, S. C. Bollin and D. J. Gardner, *Carbohydr. Polym.*, 2015, **127**, 381-389.
29. E. Lizundia, S. Petisco and J. R. Sarasua, *J. Mech. Behav. Biomed. Mater.,* 2012, **17**, 242-251.
30. J. Fernandez, A. Larranaga, A. Etxeberria and J. R. Sarasua, *J. Mech. Behav. Biomed. Mater.,* 2014, **35**, 39-50.
31. P. Scherrer, *Nachrichten von der Gesellschaft der Wissenschaften zu Göttingen, M athematisch-Physikalische Klasse*, 1918, **2**, 98-100.
32. H. M. Rietveld, *J. Appl. Crystallogr.,* 1969, **2**, 65-71.
33. J. R. Carvajal, *Physica B Condens. Matter,* 1993, **192**, 55-69.
34. J. R. Carvajal, *Commission on powder diffraction (IUCr)*, 2001, **26**, 12-19.
35. P. Hormnirun, E. L. Marshall, V. C. Gibson, R. I. Pugh and A. J. P. White, *Proc. Natl. Acad. Sci. U.S.A.,* 2006, **103**, 15343-15348.
36. S. Li, A.Girard, H. Garreau and M.Vert, *Polym. Degrad. Stab.,* 2001, **71**, 61-67.
37. M. T. Berry, D. Castrejon and J. E. Hein, *Org. Lett.,* 2014, **16**, 3676-3679.
38. D. A. Atwood, M. S. Hill, J. A. Jegier and D. Rutherford, *Organometallics*, 1997, **16**, 2659-2664.